

AD-A175 744

OBSERVATION OF STRONGLY WAVEVECTOR DEPENDENT RAMAN
SCATTERING BY LO PHONO (U) AEROSPACE CORP EL SEGUNDO
CA CHEMISTRY AND PHYSICS LAB S M BECK ET AL 30 SEP 86

1/1

UNCLASSIFIED

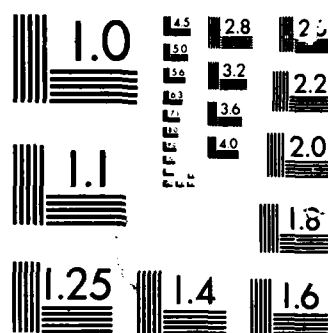
TR-8886(6945-86)-2 SD-TR-86-79

F/G 28/12

NL



1/1
2/2
3/3



AD-A175 744

Observation of Strongly Wavevector Dependent
Raman Scattering by LO Phonons
in GaAs Near the E_0 Gap

S. M. BECK and J. E. WESSEL
Chemistry and Physics Laboratory ✓
Laboratory Operations
The Aerospace Corporation
El Segundo, CA 90245

30 September 1986

Prepared for
SPACE DIVISION
AIR FORCE SYSTEMS COMMAND
Los Angeles Air Force Station
P.O. Box 92960, Worldway Postal Center
Los Angeles, CA 90009-2960

DTIC
ELECTE
JAN 07 1987
S E D

DTIC FILE COPY

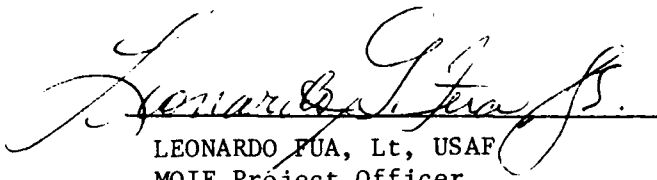
APPROVED FOR PUBLIC RELEASE:
DISTRIBUTION UNLIMITED

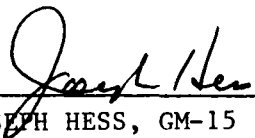
87 1 05 076

This report was submitted by The Aerospace Corporation, El Segundo, CA 90245, under Contract No. F04701-85-C-0086 with the Space Division, P.O. Box 92960, Worldway Postal Center, Los Angeles, CA 90009-2960. It was reviewed and approved for The Aerospace Corporation by S. Feuerstein, Director, Chemistry and Physics Laboratory. Lt Leonardo Fua, SD/CGXT, was the project officer for the Mission-Oriented Investigation and Experimentation (MOIE) program.

This report has been reviewed by the Public Affairs Office (PAS) and is releasable to the National Technical Information Service (NTIS). At NTIS, it will be available to the general public, including foreign nationals.

This technical report has been reviewed and is approved for publication. Publication of this report does not constitute Air Force approval of the report's findings or conclusions. It is published only for the exchange and stimulation of ideas.


LEONARDO FUA, Lt, USAF
MOIE Project Officer
SD/CGXT


JOSEPH HESS, GM-15
Director, AFSTC West Coast Office
AFSTC/WCO OL-AB



UNCLASSIFIED

SECURITY CLASSIFICATION OF THIS PAGE (When Data Entered)

REPORT DOCUMENTATION PAGE		READ INSTRUCTIONS BEFORE COMPLETING FORM
1. REPORT NUMBER SD-TR-86-79	2. GOVT ACCESSION NO.	3. RECIPIENT'S CATALOG NUMBER
4. TITLE (and Subtitle) OBSERVATION OF STRONGLY WAVEVECTOR DEPENDENT RAMAN SCATTERING BY LO PHONONS IN GaAs NEAR THE E_0 GAP		5. TYPE OF REPORT & PERIOD COVERED
		6. PERFORMING ORG. REPORT NUMBER TR-0086(6945-06)-2
7. AUTHOR(s) S. M. Beck and J. B. Wessel		8. CONTRACT OR GRANT NUMBER(s) F04701-85-C-0086
9. PERFORMING ORGANIZATION NAME AND ADDRESS The Aerospace Corporation El Segundo, Calif. 90245		10. PROGRAM ELEMENT, PROJECT, TASK AREA & WORK UNIT NUMBERS
11. CONTROLLING OFFICE NAME AND ADDRESS Space Division Los Angeles Air Force Station Los Angeles, Calif. 90009-2960		12. REPORT DATE 30 September 1986
		13. NUMBER OF PAGES 8
14. MONITORING AGENCY NAME & ADDRESS (if different from Controlling Office)		15. SECURITY CLASS. (of this report) Unclassified
		15a. DECLASSIFICATION/DOWNGRADING SCHEDULE
16. DISTRIBUTION STATEMENT (of this Report) Approved for public release; distribution unlimited		
17. DISTRIBUTION STATEMENT (of the abstract entered in Block 20, if different from Report)		
18. SUPPLEMENTARY NOTES		
19. KEY WORDS (Continue on reverse side if necessary and identify by block number) Raman scattering Gallium arsenide Stimulated Raman gain		
20. ABSTRACT (Continue on reverse side if necessary and identify by block number) Stimulated Raman gain spectra were recorded for photon energies approaching the GaAs E_0 bandgap. The results support intrinsic deformation potential and q-dependent Fröhlich scattering mechanisms, in contrast to the impurity mechanisms previously proposed to explain above-bandgap backscattering experiments.		

DD FORM 1473
(FACSIMILE)

UNCLASSIFIED

SECURITY CLASSIFICATION OF THIS PAGE (When Data Entered)

OBSERVATION OF STRONGLY WAVEVECTOR DEPENDENT
RAMAN SCATTERING BY LO PHONONS IN GaAs NEAR THE E_0 GAP

Even though Raman scattering of semiconductor materials has been studied intensively for over two decades, new experiments continue to reveal information of fundamental importance concerning the dominant mechanisms. Recent studies of GaAs suggest that impurity-induced scattering provides a major contribution to the Raman intensity observed near the $E_0 + \Delta_0$ gap, the energy range most studied (Ref. 1). Impurity-induced scattering should be independent of phonon wavevector \vec{q} and thus be observable in the forward direction (where \vec{q} is near zero), whereas intrinsic forbidden scattering should vanish in the forward direction (Refs. 2, 3). Therefore, forward scattering experiments provide a direct test of mechanisms. In prior studies of GaAs, forward scattering measurements were precluded by strong sample absorption above bandgap, or poor background laser light rejection below bandgap.

In this work we present results of forward scattering measurements at photon energies approaching, but less than, the E_0 bandgap. We report the first observation of strong symmetry selection rules for forward Raman scattering by LO phonons for parallel incident and scattered polarized light in bulk GaAs. The results demonstrate strict \vec{q} dependence and are entirely consistent with intrinsic scattering by the deformation potential (dp) and Fröhlich mechanisms. Impurity-bound exciton scattering is expected to be of maximum amplitude for our experimental conditions. Therefore the results indicate that impurity-bound exciton scattering is not important, even for doped GaAs samples.

Dipole-forbidden Raman scattering by LO phonons in semiconductor crystals is now a well-documented phenomenon (Refs. 3-5). For above-bandgap excitation, the cross-section of this scattering mechanism usually dominates that of the allowed dp mechanisms. Several years ago Martin predicted that the cross-section for the forbidden scattering should depend upon the phonon wavevector, \vec{q} (Ref. 6). In the limit of $\vec{q}=0$, dipole forbidden intensity

should vanish as a result of exact cancellation of the electron and hole contributions to the electronic-lattice (Fröhlich) interaction term responsible for the scattering. Wavevector dependent LO Raman scattering has been reported only for very pure CdS samples, but residual LO intensity was observed even for near forward scattering geometries (\vec{q} approaching zero). This was attributed to small concentrations of impurities inducing the forbidden scattering (Ref. 7).

In our experiments Raman signals were generated by the technique of stimulated Raman gain spectroscopy, using colinear pump and probe beams in a transmission geometry. Two mode-locked synchronously pumped dye lasers, independently tunable from 1.42 to 1.56 eV, provided the pump (ω_1) and probe (ω_2) frequencies (Refs. 8, 9). When $\omega_1 - \omega_2 = \omega_{LO}$, intensity was transferred from the pump beam, which was amplitude modulated at 14.2 MHz, to the probe beam. The signal was recovered from the probe beam at the modulation frequency. At 14.2 MHz, the noise associated with dye jet fluctuations was substantially reduced relative to lower frequencies (Refs. 8, 9). Sample absorption of the pump laser limited the energies to 1.51 eV or lower. Two different samples were investigated; both were 200 μm thick, cut to expose [100] faces. Sample 1 was doped with Cr (10^{17}cm^{-3}), while sample 2 was intrinsic GaAs. A liquid helium coldfinger maintained the samples at $\sim 18^\circ\text{K}$. The samples were oriented using x-ray diffraction.

Since the laser beams propagate through the sample, bulk scattering predominates and the scattering is not sensitive to electric fields present at the sample surfaces, as are above-bandgap backscattering techniques, where electric fields can strongly enhance forbidden scattering (Ref. 10). Because of the colinear geometry and the fact that the first order Raman process conserves momentum, the wavevector of the LO phonon produced by the coherent process is two orders smaller than in backscattering techniques.

The symmetry selection rules for Raman gain are the same as for spontaneous Raman scattering. Selection rules for the scattering geometries used are listed in Table I for both deformation potential and Fröhlich mechanisms. It can be seen that for parallel polarized incident and scattered

light propagating along [100], the dp allows scattering by LO phonons only for polarization along [011], and not [010], whereas the Fröhlich mechanism allows scattering for either polarization. By measuring the LO phonon Raman scattering intensity for both orientations, the two contributions can be separated.

TABLE I

SCATTERING MECHANISM	COORDINATE SYSTEM			POLARIZATION $\alpha\beta$	SELECTION RULE LO(X)
	X	Y	Z		
DP	[100]	[010]	[001]	YY or ZZ	FORBIDDEN
FRÖHLICH	[100]	[010]	[001]	YY or ZZ	ALLOWED
DP	[100]	[011]	[011]	YY or ZZ	ALLOWED
FRÖHLICH	[100]	[011]	[011]	YY or ZZ	ALLOWED

Figure 1 shows the Raman gain spectra observed near the 292 cm^{-1} LO phonon resonance for both $\vec{e}_i || \vec{e}_s || [010]$ and $\vec{e}_i || \vec{e}_s || [011]$ configurations, where \vec{e}_i and \vec{e}_s are the polarizations of the pump and probe beams respectively. The pump and probe energies are 1.481 and 1.445 eV respectively. A strong, spectrally flat, coherent signal is observed in both configurations. The ratio of Raman peak intensity to continuum signal at these excitation energies is close to 1:1. This ratio increases to about 4:1 as the pump beam energy is scanned closer to the E_0 gap. Both the continuum signal and the Raman peak show an intensity dependence on the temporal separation of the pump and probe laser pulses, which follows the cross-correlation of the two pulses. Based upon its temporal and spectral behavior,

and the relative magnitude of continuum to Raman signal, we assign the continuum signal to a coherent two-photon absorption (TPA).

Close to the bandgap, the ratio of Raman to continuum signal increases appreciably. A large out-of-phase continuum component is observed extending to longer delay times. We tentatively associate this out-of-phase component with effects due to heating or free carrier generation.

TPA is expected to be essentially isotropic, and we use the background to scale the Raman intensities for the two scattering configurations (Refs. 11, 12). The observed dependence of Raman intensity on crystal orientation, shown in Figure 1, is exactly that predicted by dp selection rules. Almost no forbidden intensity is observed, even for excitation energies only 20 meV below the E_0 bandgap. Little difference in the Raman scattering is observed for the two samples, which have vastly different impurity concentrations. The impurity induced mechanism is not restricted by momentum conservation and therefore is \vec{q} independent. Thus, we would expect to see impurity induced forward forbidden scattering if the impurity mechanism were important.

Martin's \vec{q} dependent theory of intrinsic Raman scattering provides an appropriate model for our data (Ref. 6). In Figure 2, we plot the predicted energy dependence for dp and Fröhlich scattering mechanisms, calculated for excitons plus uncorrelated free electron-hole pairs. Curve (a) represents scattering induced by the Fröhlich mechanism for the conventional backscattering geometry, (b) represents both forward and backward dp scattering, which is nearly independent of \vec{q} in the range of interest, and curve (c) presents the results for our case of forward Fröhlich induced scattering. As noted by Martin, the Fröhlich mechanism is greatly enhanced near bandgap resonance. However, because of the importance of the \vec{q} dependence for Fröhlich scattering, the theory predicts that forbidden LO near-resonant forward scattering should be undetectable in our experiment. In backward scattering at similar excitation energies, a forbidden component should be clearly evident. The exciton states cause near-resonant forbidden scattering to dominate the allowed component in backscattering geometry.

The calculations are clearly consistent with the observed near-absence of forward forbidden scattering. Impurity scattering is expected to be \vec{q} independent and would generate equivalent forbidden forward and backward scattering. The observed weak enhancement of allowed scattering with approach to bandgap resonance also supports an intrinsic mechanism; however, the present data lack the accuracy needed to quantitatively verify the theory. Therefore, the new results strongly suggest below-bandgap Raman scattering is described by dp and \vec{q} -dependent Fröhlich mechanisms. Additional studies may be needed to reconcile this with prior above-bandgap experiments (Ref. 7). Currently we are preparing to extend measurements to backscattering geometry and to use incident energies above the bandgap in order to reconcile our results with these observed for $E_0 + \Delta$ resonance conditions.

Accession For	
NTIS GEMRI	<input checked="" type="checkbox"/>
DTIC TAB	<input type="checkbox"/>
Unannounced	<input type="checkbox"/>
Justification	
By _____	
Distribution _____	
Availability Codes	
Dist _____	
A-1	

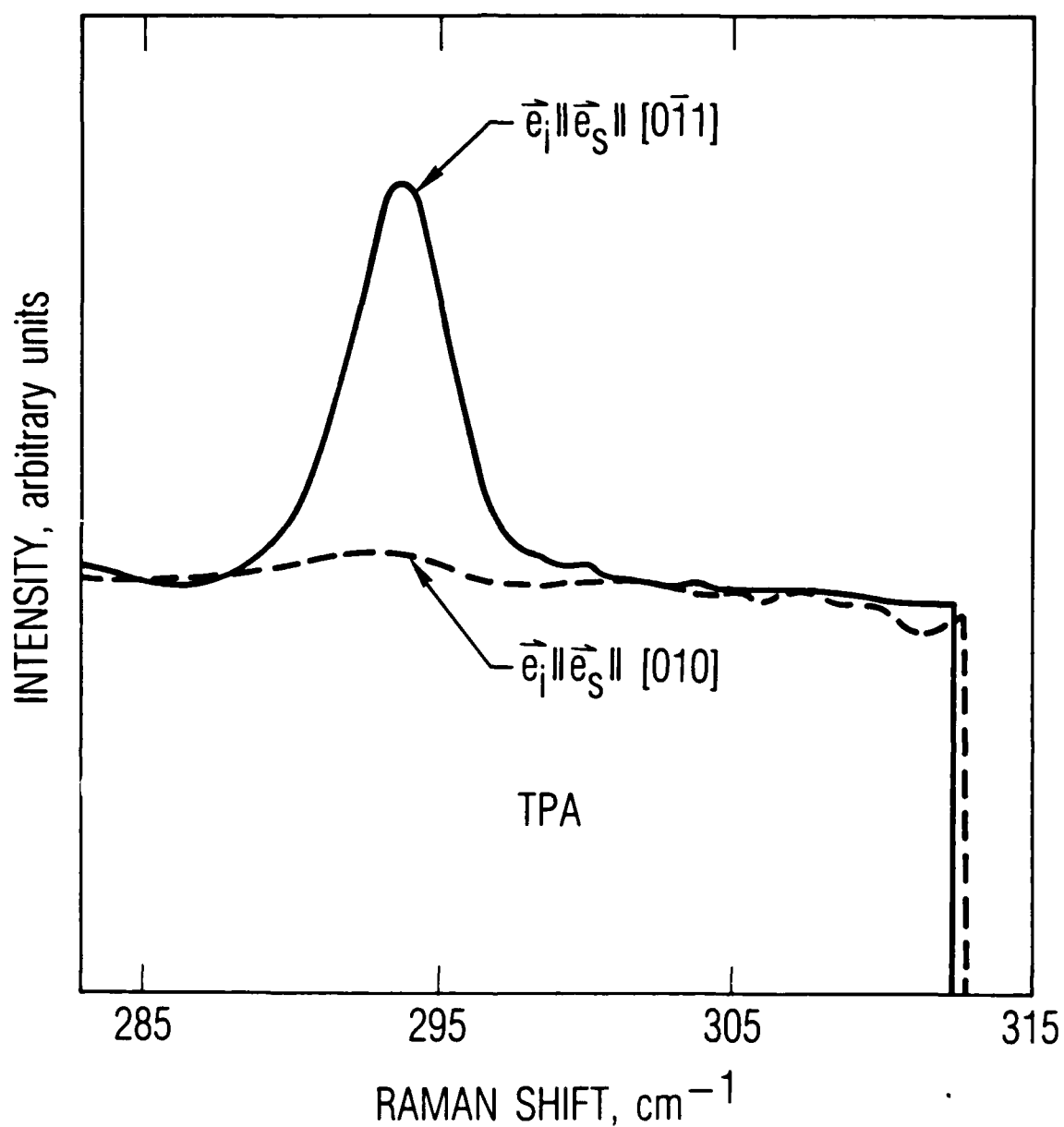


Figure 1. Raman spectrum of (100) GaAs recorded at 18K with \vec{e}_i and $\vec{e}_s \parallel [010]$ and \vec{e}_i and $\vec{e}_s \parallel [011]$, respectively. The incident photon energy was 1.481 eV, and slight enhancement of the Raman signal was observed as excitation energy approached the bandgap. The background signal is tentatively attributed to 2-photon absorption (TPA), and at higher photon energies, to heating or free carrier generation.

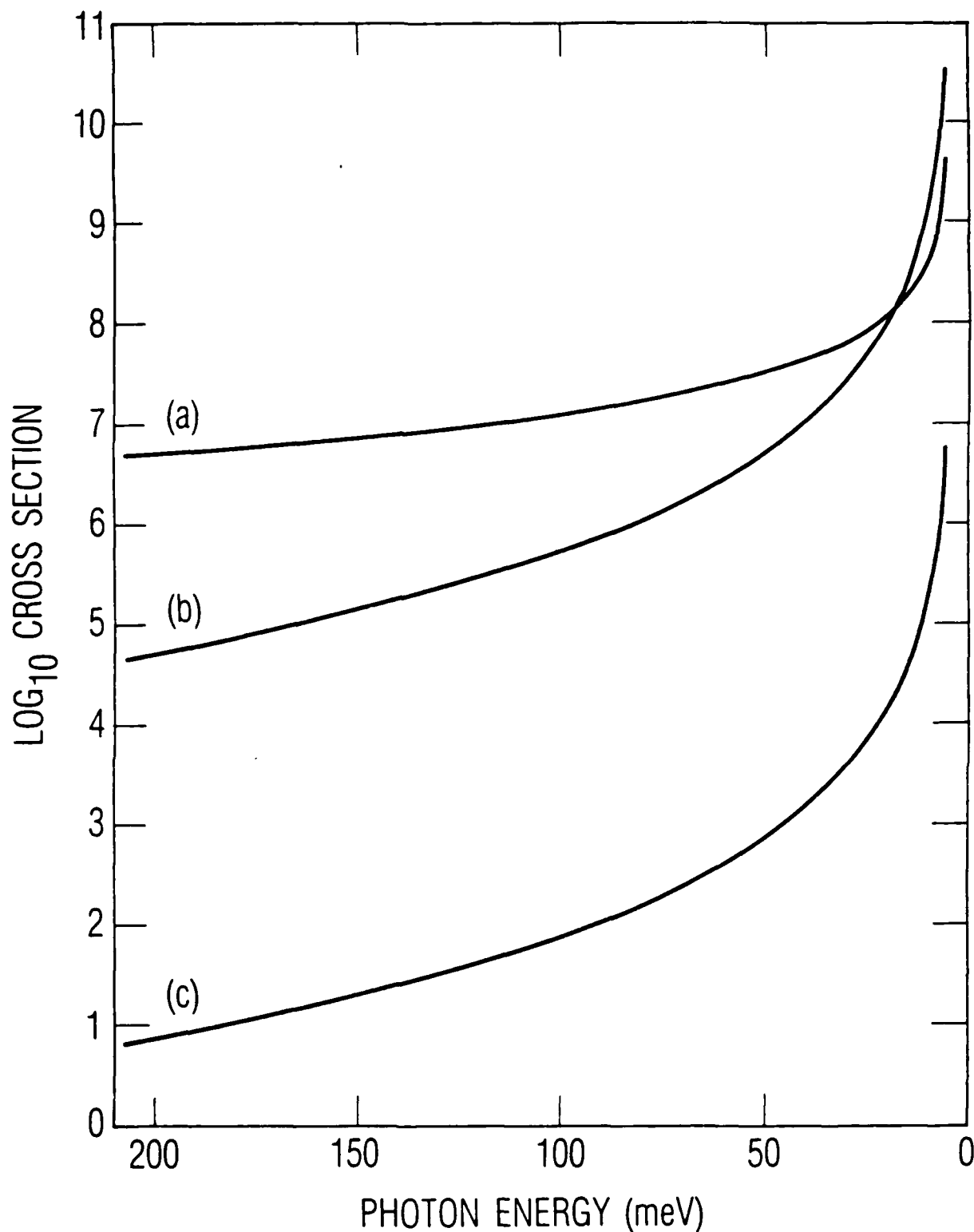


Figure 2. Raman scattering cross-sections (in arbitrary units) calculated (a) for both forward and backward scattering by the deformation potential mechanism, (b) for the Fröhlich mechanism in backward scattering with $q = 5.7 \times 10^5 \text{ cm}^{-1}$, and (c) for forward Fröhlich induced scattering, with $q = 3.6 \times 10^3 \text{ cm}^{-1}$. The photon energy is presented as $E_g - h\nu$, where E_g is the bandgap energy and ν is the photon frequency.

REFERENCES

1. José Meneéndez and Manuel Cardona, Phys. Rev. B31, 3696 (1985).
2. A. A. Gogolin and E. I. Rashba, Solid State Comm. 19, 1177 (1976).
3. R. C. C. Leite and S. P. S. Porto, Phys. Rev. Letters 17, 10 (1966).
4. A. Pinzuk and E. Burstein, Phys. Rev. Letters 21, 1073 (1968).
5. R. M. Martin and T. C. Damen, Phys. Rev. Letters 26, 86 (1970).
6. R. M. Martin, Phys. Rev. B4, 3676 (1971).
7. S. Permogorov and A. Reznitsky, Solid State Comm. 18, 781 (1976).
8. B. F. Levine and C. G. Bethea, IEEE, J. Quantum Electron, QE-16, 85 (1980).
9. J. P. Heritage, Appl. Phys. Letters 34, 470 (1979).
10. J. G. Gay, J. D. Dow, E. Burstein and A. Pinzuk, Light Scattering in Solids, M. Balkanski, ed. (1971).
11. S. J. Bepko, Phys. Rev. B12, 669 (1975).
12. J. H. Bechtel and W. L. Smith, Phys. Rev. B13, 3515 (1975).

LABORATORY OPERATIONS

The Aerospace Corporation functions as an "architect-engineer" for national security projects, specializing in advanced military space systems. Providing research support, the corporation's Laboratory Operations conducts experimental and theoretical investigations that focus on the application of scientific and technical advances to such systems. Vital to the success of these investigations is the technical staff's wide-ranging expertise and its ability to stay current with new developments. This expertise is enhanced by a research program aimed at dealing with the many problems associated with rapidly evolving space systems. Contributing their capabilities to the research effort are these individual laboratories:

Aerophysics Laboratory: Launch vehicle and reentry fluid mechanics, heat transfer and flight dynamics; chemical and electric propulsion, propellant chemistry, chemical dynamics, environmental chemistry, trace detection; spacecraft structural mechanics, contamination, thermal and structural control, high temperature thermomechanics, gas kinetics and radiation; cw and pulsed chemical and excimer laser development including chemical kinetics, spectroscopy, optical resonators, beam control, atmospheric propagation, laser effects and countermeasures.

Chemistry and Physics Laboratory: Atmospheric chemical reactions, atmospheric optics, light scattering, state-specific chemical reactions and radiative signatures of missile plumes, sensor out-of-field-of-view rejection, applied laser spectroscopy, laser chemistry, laser optoelectronics, solar cell physics, battery electrochemistry, space vacuum and radiation effects on materials, lubrication and surface phenomena, thermionic emission, photo-sensitive materials and detectors, atomic frequency standards, and environmental chemistry.

Computer Science Laboratory: Program verification, program translation, performance-sensitive system design, distributed architectures for spaceborne computers, fault-tolerant computer systems, artificial intelligence, micro-electronics applications, communication protocols, and computer security.

Electronics Research Laboratory: Microelectronics, solid-state device physics, compound semiconductors, radiation hardening; electro-optics, quantum electronics, solid-state lasers, optical propagation and communications; microwave semiconductor devices, microwave/millimeter wave measurements, diagnostics and radiometry, microwave/millimeter wave thermionic devices; atomic time and frequency standards; antennas, rf systems, electromagnetic propagation phenomena, space communication systems.

Materials Sciences Laboratory: Development of new materials: metals, alloys, ceramics, polymers and their composites, and new forms of carbon; non-destructive evaluation, component failure analysis and reliability; fracture mechanics and stress corrosion; analysis and evaluation of materials at cryogenic and elevated temperatures as well as in space and enemy-induced environments.

Space Sciences Laboratory: Magnetospheric, auroral and cosmic ray physics, wave-particle interactions, magnetospheric plasma waves; atmospheric and ionospheric physics, density and composition of the upper atmosphere, remote sensing using atmospheric radiation; solar physics, infrared astronomy, infrared signature analysis; effects of solar activity, magnetic storms and nuclear explosions on the earth's atmosphere, ionosphere and magnetosphere; effects of electromagnetic and particulate radiations on space systems; space instrumentation.

END

2-87

DTIC